

# Model of Quantum Criticality in $\text{He}^3$ bilayers Adsorbed on Graphite

A. Benlagra and C. Pépin  
 CEA, DSM, Institut de Physique Thorique, IPhT,  
 CNRS, MPPU, URA2306, Saclay,  
 F-91191 Gif-sur-Yvette, France

(Dated: November 4, 2018)

Recent experiments on  $\text{He}^3$  bilayers adsorbed on graphite have shown striking quantum critical properties at the point where the first layer localizes. We model this system with the Anderson lattice plus inter-layer Coulomb repulsion in two dimensions. Assuming that quantum critical fluctuations come from a vanishing of the effective hybridization, we can reproduce several features of the system, including the apparent occurrence of two quantum critical points, the variation of the effective mass and coherence temperature with coverage.

PACS numbers: 71.27.+a, 72.15.Qm, 75.20.Hr, 75.30.Mb

$\text{He}^3$  layers, adsorbed on graphite have attracted substantial interest since the early eighties, for their remarkable properties of surface magnetism [1, 2, 3, 4] as well as a model system for quantum wetting transitions[5]. One layer of  $\text{He}^3$  atoms adsorbed on graphite pre-plated by HD-bilayer or compressed solid has been shown to solidify at a coverage of  $4/7$  of the substrate[6, 7, 8]. This transition has been identified as a Mott transition for the  $\text{He}^3$  fermions[9]. One of the leading questions in this field has been to know whether the ground state in the Mott phase orders magnetically or is a spin liquid[6], and, in the latter case, which kind of spin liquid -gapless or gapfull- it is[7, 10]. Theoretical studies have shown that, depending on the relative strength of the ring exchange parameters[8, 11], a spin liquid phase, a canted phase, or even ferromagnetic ground state can occur. Close to the Mott transition, a gapless spin liquid ground state appears to be a reasonable choice[12]. Experimental studies of the solidification of the first  $\text{He}^3$  layer when a second or a third layer is adsorbed have been performed long ago [3, 13]. There, an enhancement of the static spin susceptibility as well as of the specific heat coefficient was observed close to the Mott transition. In the experiment [1], two layers of  $\text{He}^3$  are adsorbed on Graphite pre-plated by two layers of  $\text{He}^4$ . The originality of the data [1] lies in that it's the first system for which, when the second  $\text{He}^3$  layer arrives at promotion, the first layer is not yet solidified. As a function of the layer coverage, promotion occurs at  $n_0 \simeq 6.3nm^{-2}$  while the first layer's solidification occurs at  $n_c \simeq 9.9nm^{-2}$  (which corresponds roughly to a ratio of  $13/19$  or  $12/19$  between the first  $\text{He}^3$  layer and the  $\text{He}^4$  substrate[8]). From specific heat measurements, the effective mass is seen to be enhanced like  $m/m^* \sim \delta$ , with  $\delta = 1 - n/n_c$ , and the coherence temperature, below which the Fermi liquid behavior is recovered, is shown to decrease like  $T_{coh} \sim \delta^{1.8}$  while approaching the quantum critical point (QCP). One striking feature of the data is that, strictly speaking, the experiment doesn't reach the QCP; at  $n_1 \simeq 9.2nm^{-2}$  the specific heat behavior shows

hints of a first order transition. Moreover NMR studies show that the field-driven magnetization abruptly starts to grow at  $n = 9.2nm^{-2}$ . An activation gap extracted from the low energy behavior of the specific heat coefficient seems to vanish before the quantum critical coverage is reached. In conclusion, the phase diagram of  $\text{He}^3$  bi-layers pre-plated on two  $\text{He}^4$  layers, seems to exhibit *two* mysterious phase transitions. One at which the magnetization starts to grow, which corresponds to input of a first order transition, and one at which the ratio  $m/m^*$  and the coherence temperature curves extrapolate to zero as a function of coverage.

In this letter we model the system with the Anderson lattice in two dimensions with the addition of inter- and intra-layer Coulomb repulsion[14]. Quasi-local f-fermions are identified to the first layer  $\text{He}^3$  atoms while light c-fermions are the second layer  $\text{He}^3$  atoms. The bare hybridization corresponds to the hopping between the two layers. In the spirit of the early studies of bulk  $\text{He}^3$  [15] we solve this model for infinite Coulomb repulsion  $U$  between the f-fermions, using a slave boson technique equivalent to Gutzwiller's variational approach. The QCP of this system is identified with the Kondo breakdown QCP (KB-QCP) of the Anderson lattice[16, 17]; that is the fixed point for which the effective hybridization vanishes and, at the same time, the f-fermions localize. On the disordered side of the transition, a spin-liquid phase is necessary to stabilize the KB-QCP. We can reproduce the variations of the inverse effective mass and coherence temperature with coverage (namely  $m/m^* \simeq \delta$  and  $T_{coh} \simeq \delta^2$ ) in an intermediate temperature regime. Those variations are in good agreement with experiments, as seen in Fig.2 where we fit experimental data. While approaching the experimental critical coverage, the order parameter suddenly drops, reaching the true theoretical QCP *before* the experimental critical coverage is reached. We believe this sudden drop of the effective hybridization explains the mysterious observation that the system seems to exhibit two QCPs. Indeed, for us the true QCP is the one

at which the hybridization goes to zero, which identifies experimentally with the point where the magnetization starts to grow at  $n = 9.2nm^{-2}$ . The experimental QCP corresponds to the extrapolation to  $T = 0$  of the inverse effective mass and coherence temperature curves obtained in the *intermediate energy* regime. The drop of the order parameter obtained in our model is so abrupt that it may trigger as well first order transitions in the low energy regime.

Our starting point is the Anderson lattice model with inter- and intra-layer Coulomb repulsion:

$$\begin{aligned}
H = & \sum_{\langle i,j \rangle, \sigma} \left[ \tilde{f}_{i\sigma}^\dagger (t_{ij}^0 + E_0 \delta_{ij}) \tilde{f}_{j\sigma} \right. \\
& + \left. c_{i\sigma}^\dagger (t_{ij} - \mu \delta_{ij}) c_{j\sigma} \right] + V \sum_{i\sigma} \left( \tilde{f}_{i\sigma}^\dagger c_{i\sigma} + h.c. \right) \\
& + \sum_i (U \tilde{n}_{f,i}^2 + U_1 \tilde{n}_{f,i} n_{c,i} + U_2 n_{c,i}^2) , \quad (1)
\end{aligned}$$

where  $(i, j)$  are the lattice sites created by the Graphite's corrugate potential,  $\tilde{f}^\dagger(\tilde{f})$  are the creation (annihilation) operators for the first layer's fermions,  $c^\dagger(c)$  are the creation (annihilation) operators for the second layer's fermions,  $t_{ij} = t$  is the c-fermion's hopping taken as a constant,  $t_{ij}^0 = \alpha t$  is the f-fermion's hopping term,  $V$  is the hybridization corresponding to a hopping term between the two layers,  $E_0 < 0$  is the f-level potential and  $\mu$  is the c-fermions chemical potential. Physically, the localization of the first layer is driven by the Graphite's corrugated potential, inducing a triangular lattice in the He<sup>4</sup> bi-layers, inducing itself a second triangular lattice for the first He<sup>3</sup> layer, commensurate with the substrate's one at the "magic" filling number 13/19[8]. With respect to the "13/19" lattice, the f-fermion are thought of being close to a Mott transition; the f-band is close to half-filling and the hard core Coulomb repulsion leads to strongly correlated effects. We treat the effect of strong correlations by introducing one Coleman's slave boson [18] which decouples the  $\tilde{f}^\dagger$  creation operator at site "i" in the following way:  $\tilde{f}_{i\sigma}^\dagger \rightarrow f_{i\sigma}^\dagger b_i$  where the f-spinons and the b-holons are subject to the constraint  $\sum_\sigma f_{i\sigma}^\dagger f_{i\sigma} + b_i^\dagger b_i = 1$ . The constraint is taken into account in a Lagrangian formulation through a Lagrange multiplier  $\lambda$ . The properties of the second layer c-fermions are very close to the ones of the bulk He<sup>3</sup>[15]; the Coulomb terms  $U_1$  and  $U_2$  thus mainly re-normalize the hybridization and hopping parameters, inducing a dependence in the coverage through  $V = V_0 + V_1 n$  and  $t = t_0 + t_1 n$ , where  $n$  is the total coverage in He<sup>3</sup>.

Performing the slave boson decomposition obtains the

following Lagrangian [19]:

$$\begin{aligned}
\mathcal{L} = & \sum_{\langle i,j \rangle, \sigma} \left[ f_{i\sigma}^\dagger \left( (\partial_\tau + E_0 + \lambda) \delta_{ij} + b_i \alpha t b_j^\dagger \right) f_{j\sigma} \right. \\
& + \left. c_{i\sigma}^\dagger ((\partial_\tau - \mu) \delta_{ij} + t) c_{j\sigma} \right] \\
& + V \sum_{i\sigma} \left( f_{i\sigma}^\dagger b_i c_{i\sigma} + h.c. \right) + J \left( \sum_{\langle i,j \rangle} \vec{S}_i \cdot \vec{S}_j - n_i n_j / 4 \right) , \quad (2)
\end{aligned}$$

where  $\vec{S} = \sum_{\alpha\beta} f_\alpha^\dagger \vec{\sigma} f_\beta$  is the spin operator expressed in terms of the spinons only, with  $\vec{\sigma}$  the Pauli matrix and  $\partial_\tau$  the partial derivative in imaginary time.  $J = 2(\alpha t)^2/U$  is generated by a second order expansion of our model in  $U$ . Alternatively, the  $J$ -term can be included "ab initio" in the model in consideration of the various ring exchange parameters generated [8]. We assume that short range interactions stabilize a spin liquid with short range ferromagnetic character, in agreement with previous studies.

In order to fit the experimental data, we evaluate the dependance of the bare parameters in coverage. Following [21], we identify  $E_0$  as the difference in the average potential energy between the first and the second layer. Here, the potential energy comes from the joined effects of a) Van der Waals potential between the Graphite substrate and the layers  $V_s(z) = (4C_3^3/(27D^2)) (1/z^9 - C_3/z^3)$  where  $C_3 = 2092K\text{\AA}^3$  is the Van der Waals constant and  $D = 192K$  [8], and b) the Bernardes-Lennard Jones [20] potential acting between two He particles  $V_{LJ}(r) = 4\epsilon((\sigma/r)^{12} - (\sigma/r)^6)$  with  $\epsilon = 10.2K$  and  $\sigma = 2.56\text{\AA}$  is the hard core radius. Thus,  $E_0 = E_{l1} - E_{l2}$  with  $E_{l1} = V_s(z_1) + \sum_i \rho_i \int r dr V_{LJ}(r)$ , where  $i$  indexes the contribution from the various layers (idem for  $E_{l2}$ ). We find in Kelvin  $E_{l1} = -10.495 - 1.07 n(K)$  while  $E_{l2} = -8.73 - 0.12 n(K)$  with  $n$  the *total* coverage density in  $nm^{-2}$  in good agreement with [21]. The parameter  $E_0$  then reads  $E_0 = -1.79 - 0.95 n(K)$ . The half-bandwidths  $D_f = 2\alpha t = 2\pi/m_f$  and  $D_c = 2t = 2\pi/m_c$  are evaluated from [5] where the dependence in density is extracted from thermodynamic studies of the bulk. We find that the dependance in coverage is negligible compared to the one of  $E_0$ ;  $D_c = 1.1K$ ,  $D_f = 0.6K$  thus  $\alpha = 0.55$ . The relatively high value of  $\alpha$  is to be contrasted with the typical values obtained in standard Anderson lattice for rare earth compounds. In this system the f-band is not particularly flat compared to the c-band. The parameter  $J$  of the order of a few mK can be extracted from the experiments [1]. We take here  $J = 4mK$ . The main difficulty resides in evaluating the hybridization  $V = V_0 + V_1 n$ . Noticing that the inter-layer spacing is twice smaller than the distance between the intra-layer sites, it is reasonable to expect that the hybridization is bigger than the c- half bandwidth. In this paper we have adjusted the values of  $V_0$  and  $V_1$  to fit the experimental data. We find  $V = 13.05 - 1.2 n$ , so that at the QCP  $V_c = 1.89K$  is larger than  $D_c$ , in

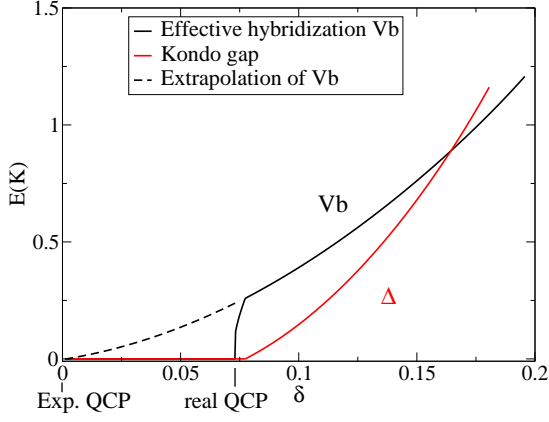


FIG. 1: Mean-field phase diagram for the Anderson lattice model in  $D = 2$  applied to  $\text{He}^3$  bi-layers. Following [1]  $\delta = 1 - n/n_c$  with  $n_c = 9.9 \text{ nm}^{-2}$ . The effective hybridization  $Vb$  drops suddenly at  $\delta = 0.072$ , indicating the real QCP. The experimental QCP is obtained by extrapolation of  $Vb$  to  $T = 0$ . The Kondo gap  $\Delta$  (in red; color online) vanishes before the real QCP.

agreement with the above observation.

The mean-field equations are obtained by making a uniform and static approximation for the holon creation (annihilation) operators  $b^\dagger(b)$  in (2), then evaluating the free energy  $F$  and solving for the two equations  $\partial F/\partial b = 0$  and  $\partial F/\partial \lambda = 0$ . We plotted in Fig.1 the effective hybridization  $bV$  as a function of the coverage (the unit for the coverage is identical to the experimental ones  $\delta = (n_c - n)/n_c$  with  $n_c = 9.9 \text{ nm}^{-2}$ ) and the “Kondo gap”  $\Delta$  defined as the energy difference between the upper band and the Fermi energy. The mean-field phase diagrams has two main features. First we observe an “elbow” in the order parameter as a function of the coverage, corresponding to the set up of the Kondo phase (strong hybridization regime). The sharp change of behavior observed corresponds to the emptying of the upper band. Note that the opening of the Kondo gap occurs at the same point. The model gives an explanation for the mysterious observation that the field-induced magnetization (or static spin susceptibility) starts to grow before the experimental QCP is reached. In our model, the point at which the magnetization starts to grow is the physical QCP, which differs from the one obtained experimentally, which corresponds to the extrapolation of the linear regime to  $T = 0$ . The static magnetic susceptibility is expected to grow quickly in as soon as the first layer localizes, since the spin liquid parameter is small  $J \sim 4 \text{ mK}$ . Moreover, from our theory the Kondo gap has to vanish *before* the QCP is reached. This comes from the observation that at half filling (corresponding to the real QCP), the f-band is half filled, hence constraining the bottom of the first layer to sit below the Fermi level. This feature is observed experimentally, if

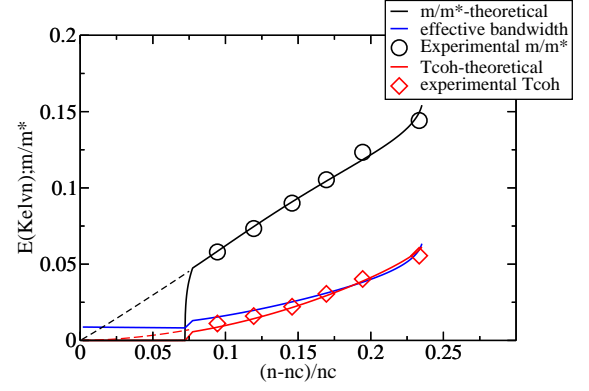


FIG. 2: Coherence temperature (K), inverse effective mass  $m/m^*$  and effective spinon bandwidth  $D_{eff} = \alpha' D_c$  (K) in the Anderson lattice model for the  $\text{He}^3$  bi-layers.  $\alpha' = b^2 \alpha + J/t$ . The dots are experimental data from [1]. The effective bandwidth sets the upper temperature of the quantum critical regime. The fitting parameters for this model are detailed in the text.

we identify the Kondo gap as the activation gap extracted from the thermodynamic measurements of [1].

The mean-field value for the QCP reads  $J/t = \exp[E_0 D_c/V^2]$  as in [17]. We understand that any small variation in the value of  $V$  with coverage has an exponential impact on the position of the QCP, justifying our option of adjusting the value of  $V$  to fit the data.

We now turn to the fluctuations. A striking observation inferred from the experimental data, is the absence of quantum critical (QC) regime in temperature. A Curie law for the spin susceptibility is observed at very low temperatures in the localized phase and directly above  $T_{coh}$ . Generically, the upper energy scale of the QC fluctuations is determined by the first irrelevant operator. In our model the formation of the spin liquid and of the Fermi liquid are the two mechanisms for quenching the entropy. Hence the temperature  $T^*$  below which the entropy  $R \ln 2$  is quenched goes like  $\text{Max}[D_{eff}, T_{coh}]$ , with  $D_{eff}$  the effective bandwidth of the spinons and  $T_{coh}$  the coherence temperature coming from the quantum fluctuations. The dependence of  $D_{eff}$  and  $T_{coh}$  with coverage are depicted in Fig 2. We see that  $D_{eff}$  is of the order of  $J \sim 4 \text{ mK}$  in the localized phase and follows  $T_{coh}$  in the Fermi liquid phase. The fact that  $J$  in this system is a remarkably small energy scale, compared to heavy fermions, is thus the reason why the QC regime is reduced to much lower temperatures. Quantum fluctuations are thus most clearly seen through the variation of the effective mass and the shape of  $T_{coh}$ .

The quantum fluctuations are in the same universality class as the ones of the Kondo breakdown model [17]. The fluctuation spectrum in the intermediate energy regime admits the dynamical exponent  $z = 3$ ,

$$D_b^{-1}(q, \Omega_n) = D_0^{-1} \left[ q^2 + \xi^{-2} + \frac{\gamma |\Omega_n|}{\alpha' q} \right], \quad (3)$$

with  $D_0 = 4k_F^2/(\rho_0 V^2)$ ,  $\xi$  is the correlation length associated with the fluctuations of  $b$ ,  $\gamma = mV^2 D_0/(\pi v_F)$ ,  $\alpha' = b^2 \alpha + J/t$  and  $\rho_0 = m_c/(2\pi)$  is the c-fermions density of states. The boson mass is given by  $m_b = D_0^{-1} \xi^{-2}$  evaluated at  $T = 0$ . We evaluate it by differentiating twice the mean-field equations with respect to the bosonic field  $b$  and evaluating the result at the mean-field saddle point. For the effective mass, we use the Luttinger-Ward expression of the free energy typical of Heisenberg-type theories, analogous to the one derived in [22]  $F = F_{FG} + T/2 \sum_n \int d^2 q/(2\pi)^2 \log [D^{-1}(q, \Omega_n)]$  where  $F_{FG}$  is the free-energy of the system at the mean-field. Since the system at the mean-field consists of two hybridized bands, one obtains after diagonalization

$$F = -\frac{\pi T^2}{6} \left[ 2\pi(\rho_1 + \rho_2) + \frac{\gamma \xi}{4\alpha'} \right], \quad (4)$$

where  $\rho_1(\rho_2)$  are the density of states of the upper(lower) bands. The effective mass thus reads  $m^* = 2\pi(\rho_1 + \rho_2) + \gamma \xi/(4\alpha')$ . The coherence temperature is computed by evaluating the corrections to scaling to the boson propagator (3); namely the one loop diagrams responsible for the temperature dependence of  $m_b(T) = D_0^{-1} \xi^{-2}(T)$ . Following [23] we find (remember  $z = 3$  here)

$$m_b(T) = m_b(T = 0) + C T \text{Log} T, \quad (5)$$

where  $C$  had to be adjusted to  $C = 7.5 \cdot 10^{-3}$  to fit the data, while the analytic evaluation gives  $C = DJ/(6V_c^2)$ . The coherence temperature  $T_{coh}$  obtains when the cross-over condition  $m_b(T) = 0$  is satisfied. The results for  $m/m^*$  and  $T_{coh}$  are presented in Fig.2 and directly compared to experiments. Since we work within a slave boson saddle point approximation, the need of one fitting parameter for the amplitude of the coherence temperature is to be expected. The exponents can be understood in a simple way. For  $z = 3$  theories in the Fermi liquid phase, the effective mass goes like the correlation length [23]  $m/m^* \sim \xi^{-1}$ . From the dispersion of the boson mode we see that  $\xi^{-1} \sim \sqrt{m_b} \sim b$ . Now the coherence temperature goes like  $b^2$ . In the regime where  $b$  varies linearly with the coverage  $n$  we thus get

$$m/m^* \sim cst - n, \quad T_{coh} \sim (cst - n)^2. \quad (6)$$

In conclusion we have performed a study of quantum criticality in  $\text{He}^3$  bi-layers by mapping the experiments on an extended version of the Anderson lattice in two dimensions. We examined the possibility for the Kondo breakdown QCP to be responsible for the quantum fluctuations observed. The system of  $\text{He}^3$  bi-layers enables to directly test the theory from the bare parameters. Our model is successful in that

- it explains the occurrence of two QCPs seemingly observed experimentally. Our interpretation is that one of the QCPs observed experimentally corresponds to the extrapolation to  $T = 0$  of an intermediate energy regime;

- it predicts that the activation gap extracted from thermodynamic measurements vanishes before the QCP is reached;
- it gives exponents for the variation of the effective mass  $m/m^*$  and the coherence temperature  $T_{coh}$  in good agreement with experiment, so that a direct fitting of the data is possible.

We have used three fitting parameters to account for the prefactors of the effective mass and coherence temperature as well as to precisely determine the position of the QCP from the bare parameters. Our study is the first case where an itinerant QCP showing non Fermi liquid behavior is used to fit experimental data from the bare parameters.

Useful discussions with H. Godfrin, G. Misguich, M. Neumann, J. Nyéki, O. Parcollet, M. Roger and J. Saunders are acknowledged. This work is supported by the French National Grant ANR26ECCEZZZ.

- 
- [1] M. Neumann *et al.*, Science **317**, 1356 (2007)
  - [2] H. Franco, R. E. Rapp and H. Godfrin, Phys. Rev. Lett. **57**, 1161 (1986).
  - [3] D. Greywall, Phys. Rev. B **41**, 1842 (1990).
  - [4] M. Siqueira *et al.* Phys. Rev. Lett. **78**, 2600 (1997).
  - [5] L. Pricapenko and J. Treiner, Phys. Rev. Lett **72**, 2215 (1994).
  - [6] K. Ishida *et al.* Phys. Rev. Lett. **79**, 3451 (1997).
  - [7] E. Collins *et al.* Phys. Rev. Lett. **86**, 2447 (2001).
  - [8] M. Roger, C. Bäuerle, H. Godfrin, L. Godfrin and J. Treiner, J. Low Temp. Phys. **112**, 451 (1998).
  - [9] A. Casey *et al.* Phys. Rev. Lett. **90**, 115301 (2003).
  - [10] R. Masutomi *et al.* Phys. Rev. Lett. **92**, 025301 (2004).
  - [11] M. Roger, Phys. Rev. Lett. **64**, 297 (1990).
  - [12] G. Misguich, P. Bernu, C. Lhuillier and D. Waldtmann, Phys. Rev. Lett **81**, 1098 (1998).
  - [13] K.-D. Morhard, C. Buerle, J. Bossy, Y. Bunkov, S.N. Fisher and H. Godfrin Phys. Rev. B **53**, 2658 (1996).
  - [14] A. Hewson, in *The Kondo problem to heavy fermions*, Cambridge U. Press, page 333.
  - [15] D. Vollhardt, Rev. Mod. Phys. **56**, 99 (1984).
  - [16] T. Senthil, S. Sachdev and M. Vojta, Phys. Rev. Lett. **90**, 216403 (2003).
  - [17] I. Paul, C. Pépin and M. Norman cond-mat/0605152; C. Pépin cond-mat/0610846.
  - [18] P. Coleman, Phys. Rev. B **29**, 3035 (1984).
  - [19] The renormalized f-band chemical potential equals the c-band's one, ensuring chemical equilibrium.
  - [20] N. Bernardes, Phys. Rev. **120**, 1927 (1960).
  - [21] S. Tasaki, Prog. Theor. Phys. **79**, 1311 (1988).
  - [22] A.V. Chubukov, D. L. Maslov *et al* Phys. Rev. B **71**, 205112 (2005) (appendix C)
  - [23] J. Rech, C. Pépin and A.V. Chubukov, Phys. Rev. B **74**, 195126 (2006).